TECHNOLOGIES AND TECHNIQUES

Advances in whole-embryo imaging: a quantitative transition is underway

Periklis Pantazis[1] *and Willy Supatto*[2]

Abstract | With the advent of imaging probes and live microscopy, developmental biologists have markedly extended our understanding of the molecular and cellular details of embryonic development. To fully comprehend the complex mechanistic framework that forms the developing organism, quantitative studies with high fidelity in space and time are now required. We discuss how integrating established, newly introduced and future imaging tools with quantitative analysis will ensure that imaging can fulfil its promise to elucidate how new life begins.

Confocal microscopy
An optical imaging technique that uses point-scanning illumination and a spatial pinhole to obtain optical sectioning and to eliminate out-of-focus signals in tissue.

Two-photon microscopy
An optical imaging technique that uses point-scanning illumination, a near-infrared spectrum femtosecond laser and two-photon absorption to obtain optical sectioning and improved imaging depth compared with confocal microscopy.

[1]*Department of Biosystems Science and Engineering (D-BSSE), Eidgenössische Technische Hochschule (ETH) Zurich, 4058 Basel, Switzerland.*
[2]*Laboratory for Optics and Biosciences, École Polytechnique, Centre National de la Recherche Scientifique (CNRS) UMR7645, and Institut National de la Santé et de la Recherche Médicale (INSERM) U696, 91120 Palaiseau, France.*
e-mails: periklis.pantazis@bsse.ethz.ch; willy.supatto@polytechnique.edu
doi:10.1038/nrm3786
Published online 16 April 2014

One of the major accomplishments of studies in embryology and genetics has been the introduction of preserved concepts of development across species. In particular, studies carried out in the fruitfly *Drosophila melanogaster*[1,2] and the worm *Caenorhabditis elegans*[3] have provided a mechanistic framework for how cellular diversity and order are achieved in individual organisms. The introduction of fluorescent imaging has greatly benefited the study of fundamental questions that concern differentiation, pattern formation and growth control. The use of live animal imaging to follow the form and function of cells and of tissues has uncovered the intricate processes of development. Such insights are beginning to challenge the established models and lead to a new understanding of embryonic development (reviewed in REFS 4–7).

However, to elucidate the elaborate cell dynamics (cell division, motility and morphological changes) and protein dynamics (turnover and kinetics of key factors) that underlie development, biologists are increasingly recognizing the need to carry out quantitative imaging with high spatiotemporal resolution from the single-cell level to that of the entire organism. This endeavour will greatly benefit from the rapid development of fluorescent protein engineering (reviewed in REF. 8) and, potentially, from the synthesis of various nanocrystals that provide increased photostability in combination with decreased background noise in the highly light-scattering environment of a whole-animal preparation. Similarly, the optical design of microscopes has markedly evolved, from standard confocal microscopy and two-photon microscopy to light-sheet microscopy that can capture the development of an entire embryo, one cell at a time. These advances have posed new challenges for image processing and quantitative analyses for which promising solutions are emerging. With such a rapid introduction of a multitude of new and improved imaging tools, it comes as no surprise that biologists are often confused with regard to which tools are relevant and appropriate for their particular application.

In this Review, we provide an overview of how, over the past decade, advances in imaging probes, microscopy techniques and image analysis have enabled quantitative studies that made it possible to gain a deeper knowledge and understanding of the dynamic processes of embryonic differentiation, patterning and morphogenesis (FIG. 1). Furthermore, we emphasize the limitations of currently available approaches and provide an outlook of how new discoveries and developments might affect the field of quantitative whole-animal imaging.

Genetically encoded fluorescent probes

Advances in synthetic chemistry, material sciences and molecular genetics have resulted in many optical tags that have enabled non-invasive imaging in living organisms to investigate the dynamics of developmental processes. In particular, the cloning[9] and expression[10] of GFP from the jellyfish *Aequorea victoria* and the subsequent development of various genetically encoded fluorescent proteins have introduced powerful and versatile tools that have provided unprecedented insights into the complex framework of a developing organism. The ease of expressing fluorescently tagged proteins or obtaining fluorescently marked cell populations by straightforward genetic means (such as the use of a tissue-specific promoter or random gene insertion) has enabled various quantitative imaging applications, which have revealed a wealth of information with regard to the function and behaviour of many biological processes. The currently available fluorescent proteins can be divided into three categories: non-modifiable, photoactivatable and photoconvertible proteins.

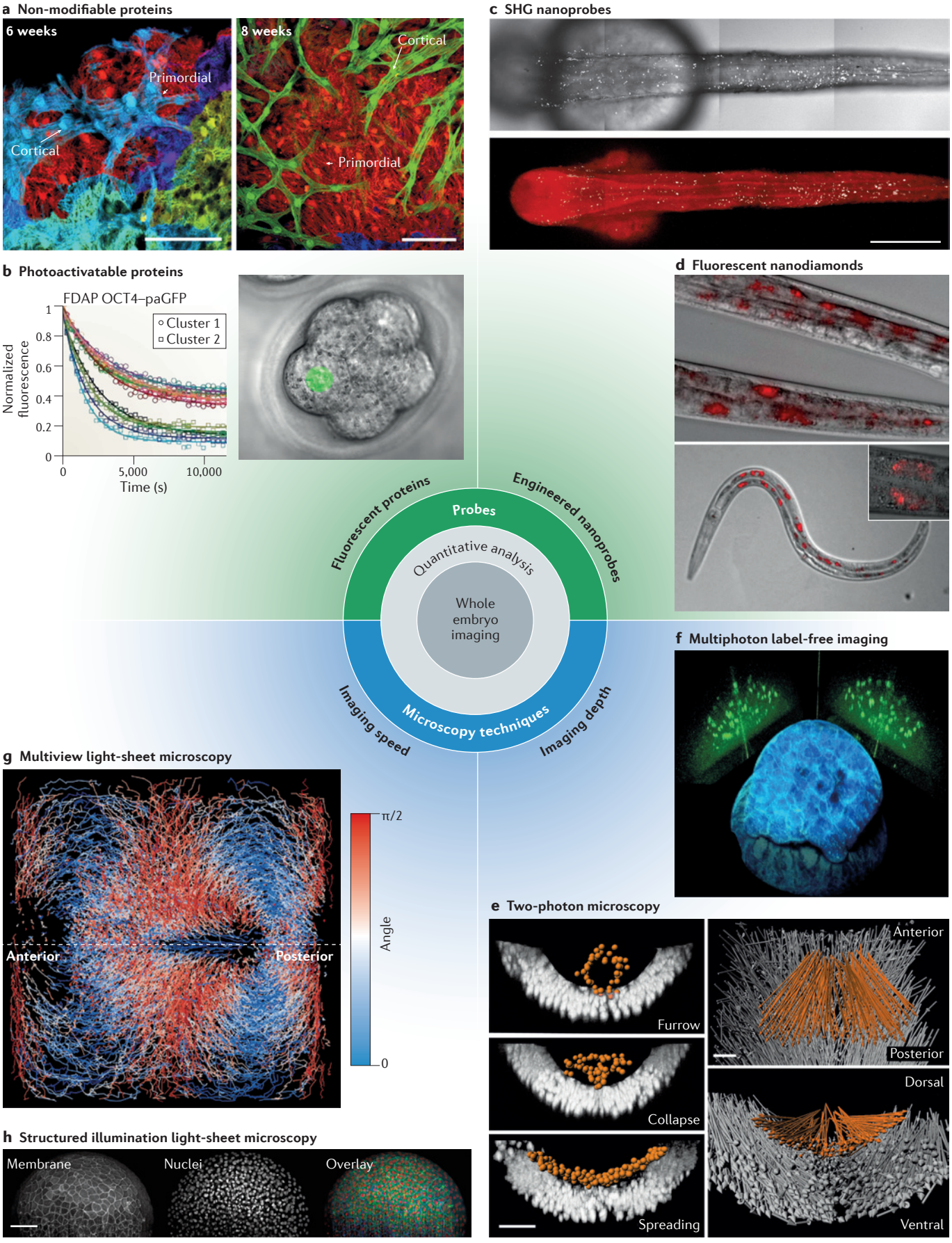

Figure 1 | **Imaging probes and microscopy techniques for quantitative whole-embryo imaging.** **a** | Non-modifiable fluorescent proteins. Ventricular surface examined in 6- and 8-week-old zebrafish that had undergone 'Brainbow' labelling of cardiomyocytes at 2 days post-fertilization, with cortical (arrow) and primordial (arrowhead) muscle indicated. Scale bar, 50 µm. **b** | Photoactivatable fluorescent proteins. Photoactivation of octamer-binding 4 (OCT4)–photoactivatable GFP (paGFP) in a single-cell nucleus of a developing mouse embryo in combination with resulting fluorescence decay after photoactivation or photoconversion (FDAP) curves for OCT4–paGFP that were obtained from data from several cell nuclei of pre-compacted four-cell and eight-cell stage embryos. **c** | Second harmonic generation (SHG) nanoprobes. Pegylated (using polyethylene glycol) barium titanate SHG nanoprobes (white) persist within cells throughout the body of the zebrafish after 24 hours of development (BODIPY TR methyl ester-stained zebrafish shown in red). Scale bar, 300 µm. **d** | Fluorescent nanodiamonds. Epifluorescence and differential interference contrast merged images of wild-type *Caenorhabditis elegans* that were fed with bioconjugated fluorescent nanodiamonds. **e** | Two-photon microscopy. Deep-tissue imaging using two-photon excited fluorescence microscopy to follow the dynamics of mesodermal cell spreading (orange) on top of the ectodermal cell layer (grey) during gastrulation of fly embryos. Scale bars, 20 µm. **f** | Multiphoton label-free imaging. Three-dimensional, label-free imaging of an early zebrafish embryo using SHG signals from mitotic spindles (green) and third harmonic generation (THG) signals from cell–cell interfaces (blue) to track cells and their divisions, and to reconstruct the lineage tree. **g** | Multiview light-sheet microscopy. A map of endodermal cell dynamics around gastrulating zebrafish embryos using multiview light-sheet microscopy and real-time image processing of multiple embryos in parallel. The colour code indicates the unsigned angle between the cell track and dorsal midline. **h** | Structured illumination light-sheet microscopy. Improved membrane imaging of a zebrafish embryo using structured illumination light-sheet microscopy. Images of membranes (left and green) were acquired using structured illumination to improve contrast. Images of nuclei (middle and red) were recorded with standard light-sheet microscopy. Scale bar, 100 µm. Part **a** from REF. 26, Nature Publishing Group. Part **b** from REF. 31, Nature Publishing Group. Part **c** from REF. 66, Nature Publishing Group. Part **d** reprinted with permission from REF. 45, American Chemical Society. Part **e** reprinted with permission from REF. 72, American Association for the Advancement of Science. Part **f** reprinted with permission from REF. 79, American Association for the Advancement of Science. Part **g** from REF. 96, Nature Publishing Group. Part **h** from REF. 102, Nature Publishing Group.

Light-sheet microscopy
An optical imaging technique whereby the specimen is illuminated with a sheet of light perpendicular to the detection direction, which provides excellent sectioning capabilities, fast imaging and low levels of photodamage.

Fluorescence recovery after photobleaching
(FRAP). An imaging assay that can determine the diffusion properties of labelled molecules in a tissue by photobleaching a small defined fluorescent region, which is followed by measuring the rate and extent of fluorescence recovery emanating from neighbouring regions.

Fluorescence correlation spectroscopy
(FCS). An imaging assay that can determine the diffusion properties of labelled molecules in a tissue by measuring fluorescence fluctuations in a small volume.

Non-modifiable proteins. Among all of the non-modifiable variants, the monomeric version of enhanced GFP (eGFP)[11] has proved, with its well-characterized photophysical behaviour, to be the most suitable option for obtaining quantitative data in developing embryos. The movement of fluorescent proteins can be monitored in either a large-scale volume using fluorescence recovery after photobleaching (FRAP)[12] or in a small-scale volume using fluorescence correlation spectroscopy (FCS)[13]. Both approaches have been successfully used to measure the distribution, diffusion and clearance of eGFP-labelled morphogens during embryogenesis. By combining sophisticated imaging with *in silico* modelling, several groups have investigated the mechanisms that control the formation of morphogen gradients, thereby revealing unexpected complexities of morphogen dispersal[14–20]. Using tissue-level FRAP in zebrafish embryos, one study showed that differential diffusivity is the major determinant of the range differences between the morphogens Nodal and Lefty (also known as left-right determination factor 1); in other words, Lefty proteins move more quickly away from the source than do Nodal proteins[18]. Similarly, another study used point FCS in zebrafish embryos to show that fibroblast growth factozr 8 (Fgf8) spreads by extracellular diffusion and that the gradient is formed by endocytosis-mediated clearance of Fgf8 from the extracellular space. Interestingly, this study identified a second, minor group of Fgf8 that is probably associated with carbohydrates located at the cell surface, as it had a tenfold lower diffusion coefficient[16]. However, it is unknown how both observable pools of Fgf8 (extracellular and cell surface-associated) interact over long timescales to yield the long-range tissue-level behaviour. To deduce global regulation mechanisms from local experiments in a living organism, which constantly undergoes shape and position changes that are caused by tissue growth and morphogenesis, will require a volumetric FCS approach with good spatial and temporal resolution in three dimensions. The implementation of FCS in a light-sheet microscope (see below) is poised to address this issue; for example, this technique has recently enabled FCS recordings of microspheres that were injected into the zebrafish blood circulation system[21] and of protein diffusion in fly wing imaginal discs[22].

To reveal the cell and population dynamics that occur during various developmental processes, non-modifiable fluorescent proteins are increasingly being used in multicolour-tracing approaches[23–25]. For example, a recently described cell-labelling technique used random Cre–*loxP* recombination to express varied combinations of spectrally distinct fluorescent proteins (such as red, yellow and cyan fluorescent proteins) in neighbouring cells, thereby creating a 'rainbow' of colours that can be followed over extended time periods[23]. Originally developed to distinguish individual neurons in the mouse brain (a 'Brainbow')[23], this method has been recently adapted to map individual cell and population dynamics in heart morphogenesis during zebrafish development. By simultaneously following the descendants of individual cells that were labelled with fluorescent proteins of different colours, one study unexpectedly found that only a small number of 'clonally dominant' founder cells function to modify the architecture (in this case, thickening of the ventricular wall) of the adult zebrafish heart[26] (FIG. 1a). Similarly, the authors of another study induced rainbow-labelled clones in early mammalian embryos to determine the contribution of individual blastomeres to embryonic and extra-embryonic lineages at the blastocyst and post-implantation stages. They observed a significant bias in the contribution of the labelled clones to the trophectoderm or the inner cell mass in a subset of mouse embryos[27]. Although the Brainbow method has provided impressive insights into cell dynamics, it has disadvantages. In contrast to other approaches with precise and rapid cellular targeting abilities, such as the recently introduced PhOTO zebrafish (photoconvertible optical tracking of zebrafish)[28], the Cre–*loxP* recombination event does not lead to instantaneous cell labelling, which makes precise spatiotemporal tracking of a cell population from the clonal founder challenging. Following genetic rearrangement, spectrally distinct fluorescent signatures manifest with a marked time lag that depends on the maturation of the newly produced fluorescent proteins and on the turnover kinetics of fluorescent proteins when they are uncoupled from production; however, once established, such labelling is permanent.

Box 1 | **Increased imaging depth in multiphoton microscopy**

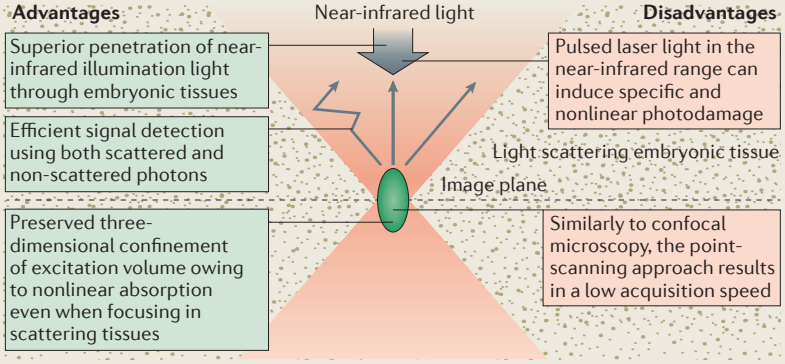

Imaging depth is limited by both scattering and absorption of visible light. When imaging deep inside embryos, light scattering compromises the illumination and the fluorescence detection, which results in degraded spatial resolution and increased background noise[69]. Deeper imaging is obtained by exciting within the so-called 'optical transparency window' (between wavelengths of 650 nm and 1,200 nm) owing to the minimal scattering of near-infrared light and minimal absorption by biological molecules (see the figure). This spectral region also provides decreased autofluorescence. Compared with other fluorescence microscopy techniques, the efficiency of multiphoton microscopy for deep-tissue imaging relies on three unique features: superior penetration of near-infrared illumination light; preserved three-dimensional confinement of the excitation volume even when focusing inside a scattering medium; and efficient collection of the fluorescence using both non-scattered and scattered photons. The optical sectioning in multiphoton microscopy is achieved by three-dimensional confinement of the multiphoton process within the focal volume. Therefore, the emitted signal is known to originate from this volume only, and all photons can be collected without requiring a pinhole to reject out-of-focus emission and scattered photons, as is required in confocal microscopy. As a consequence, and unlike most microscopy techniques, scattered and emitted photons contribute to the signal in multiphoton microscopy: this collection efficiency is a distinctive feature of multiphoton microscopy for deep-tissue imaging.

Morphogens
Signalling molecules that are typically present in gradients and that determine where specific cell types form in developing tissues.

PhOTO zebrafish
(Photoconvertible optical tracking of zebrafish). A transgenic zebrafish line with life-long fluorescent labelling of nuclear or plasma membrane proteins using the photoconvertible protein Dendra2. Taking advantage of the instantaneous photoconversion of the Dendra2 fusion protein, the non-invasive, targeted and high-contrast selection of any cells of interest can be accomplished, which greatly simplifies cell segmentation and tracking in time and space.

Photoactivatable and photoconvertible proteins. Among the recent increase in number of available monomeric photoactivatable and photoconvertible fluorescent proteins (reviewed in REF. 8), only photoactivatable GFP (paGFP)[29] and green-to-red photoconvertible Dendra2 (REF. 30) have been used to carry out quantitative whole-embryo imaging[18,20,31,32]. Taking advantage of localized multiphoton photoactivation of paGFP[33], a recent study used fluorescence decay after photoactivation or photoconversion (FDAP) to analyse the kinetics of octamer-binding 4 (OCT4; also known as POU5F1), a key transcription factor that controls pre-implantation development, in individual nuclei of a developing mammalian embryo (FIG. 1b). FDAP measurements led to the discovery of two cell populations with distinct OCT4 kinetics before any morphological differences were noticeable. These findings identified that transcription factor kinetics, rather than expression levels, are a measure of developmental heterogeneity that predicts cell lineage patterning in the early mouse embryo[31,34]. Comparably, FDAP measurements of Dendra2-tagged morphogens Nodal and Lefty were carried out in zebrafish to determine their half-life after photoconversion. By monitoring the degradation of the irreversibly photoconverted Dendra2-tagged proteins, the authors showed a lack of differential clearance between Nodal and Lefty that could not therefore account for the difference in their ranges[18]. Although FDAP with photoconvertible proteins is generally preferred over the use of photoactivatable proteins — as photoconvertible proteins combine the strength of global analysis of the non-converted population with sparse or partial analysis of the photoconverted population — multiphoton excitation of photoconvertible proteins for spatially confined analysis in whole-animal imaging has not yet been accomplished.

The present set of fluorescent proteins has given researchers an unprecedented variety for use in quantitative imaging assays, but there are many areas in which further improvement is required. Developmental biologists would like to peer more deeply into living animals. Imaging depth is, however, limited by both the scattering and absorption of visible light in tissue (BOX 1). Efforts have recently been made to engineer GFP-like fluorescent proteins with emission and excitation spectra at near-infrared wavelengths, which undergo substantially less light scattering and absorption than visible light in most tissues[35–38]. However, the brightness of current proteins with near-infrared emission and excitation spectra fails to match the specifications of monomeric GFP. Another promising template for engineering fluorescent proteins with emission and excitation spectra at near-infrared wavelengths is the bacterial phytochrome photoreceptor subfamily. To fluoresce, these photoreceptors bind the fluorophore biliverdin, a ubiquitous intermediate of haem metabolism in mammalian tissues. As these photoreceptors have the most red-shifted spectra of all the available fluorescent probes, a marked improvement in signal power has been reported in deep-tissue imaging, and using such photoreceptors is poised to offer substantial advantages for live-animal imaging[39–43].

Engineered nanoprobes

Another limitation of the currently available fluorescent probes is that in many experimental settings they fall short of their potential owing to photobleaching (permanent loss of signal) and to signal saturation (the finite number of photons that can be emitted in a given time) of the dye. To address this challenge, various nanoprobes are being developed for *in vivo* animal imaging (TABLE 1): quantum dots[44], fluorescent nanodiamonds[45,46], upconverting nanoparticles[47,48], surface-enhanced Raman scattering (SERS) nanoparticles[49] and second harmonic generation (SHG) nanoprobes[50] (FIGS 1c,d). Their successful application to whole-embryo imaging and cell and molecular tracking experiments has not yet been proven in all cases, but their potential in this respect merits further research.

Quantum dots. These fluorescent inorganic nanocrystals of 2–8 nm in diameter (up to 20 nm in diameter when surface-coated) typically consist of a core of one semiconducting material (such as cadmium selenide (CdSe)) that is surrounded by a shell of another semiconducting material (such as zinc sulphide (ZnS)) (reviewed in REF. 51).

Table 1 | **Properties to consider when choosing imaging probes for whole-embryo imaging**

Properties	Genetically encoded fluorescent proteins	Quantum dots	Fluorescent nanodiamonds	Upconverting nanoparticles	Surface-enhanced Raman scattering (SERS) nanoparticles	Second harmonic generation (SHG) nanoprobes
Genetically encoded	Yes	No	No	No	No	No
Size	~5 nm	2–20 nm	≥5 nm	≥5 nm	≥50 nm	≥20 nm
Photobleaching	Yes	No*	No	No	No	No
Blinking	Yes	Yes‡	No	No	Yes	No
Tissue toxicity	No	No§	No	No§	No	No
Proven successful multi-marker imaging (can also be used in combination with fluorescent proteins)	Yes (NA)	Yes (Yes)	No (No)	Yes (Yes)	Yes (Yes)	Yes‖ (Yes)
Interference from background tissue autofluorescence	Yes	Yes¶	Yes¶	No	Yes#	No
Depth-independent spectra**	No	No	No	No	Yes	Yes
Proven *in vivo* molecular targeting (and molecular tracking)	Yes (Yes)	Yes (Yes)	Yes (No)	Yes (No)	Yes (No)	No (No)

NA, not applicable. *Signal decay occurs under strong laser illumination. ‡Blinking has been markedly reduced in cadmium zinc selenide/zinc sulphide (CdZnSe/ZnS) quantum dots[125]. §Quantum dots and upconverting nanoparticles require a surface coating to avoid tissue toxicity. ‖Relative SHG signal intensities from at least two distinct frequencies of illumination need to be compared to distinguish different SHG nanoprobe materials for a multi-SHG imaging modality[50]. ¶Given that quantum dots and fluorescent nanodiamonds have a substantially longer fluorescence lifetime than that of endogenous autofluorescence, a separation can be accomplished using fluorescence lifetime imaging microscopy (FLIM). #Although each signal peak is narrow, a wide-spectrum intensity profile is required to acquire the characteristic spectrum of the SERS nanoparticle. **The signal is lost at lower wavelengths, as the extent of tissue light absorption and scattering decreases with increasing wavelength.

When the core is excited by a photon, the nanocrystal emits light as it returns to the ground state. Quantum dot conjugates have been successfully used for various applications in live-animal targeting and imaging[52,53] and even for molecular tracking[54]. They have several unique optical properties that are highly desirable for *in vivo* imaging: the narrow emission wavelength of quantum dots can be precisely tuned by the size of the quantum dots — from the ultraviolet spectrum to the near-infrared spectrum; and the excellent long-term photostability is paired with a large light absorption cross section for two-photon microscopy, which renders them very bright for deep-tissue imaging applications. However, most quantum dots are composed of heavy metals that are known to be toxic in their soluble form.

Fluorescent nanodiamonds. Fluorescence from nanodiamonds results from crystal defects that consist of a single nitrogen atom next to a 'missing' carbon atom (reviewed in REF. 55). Such 'nitrogen vacancy' centres are extremely photostable and show no photobleaching or blinking unless they are incorporated into small diameter (<5 nm) nanodiamonds[56]. As nanodiamonds fluoresce in the near-infrared spectrum with limited light scattering and absorption in tissue (BOX 1), and have exceptional biocompatibility, they are beginning to be used as probes for *in vivo* cell and molecular targeting and imaging[57] (FIG. 1d). However, the wide, single-band emission spectra of fluorescent nanodiamonds provides a challenge for multi-label imaging.

Upconverting nanoparticles. These are inorganic ceramic particles of 5–50 nm in diameter in which rare earth elements are embedded in a crystalline matrix (reviewed in REF. 58). Lanthanide ions are typically used to increase fluorescence and function as luminescent centres. Fluorescence from such nanoparticles is caused by a nonlinear process in which the sequential absorption of, for example, two photons in the near-infrared spectrum leads to the emission of light at shorter wavelengths. In contrast to other emission processes resulting from multiphoton excitation, upconverting nanoparticles can be efficiently excited even at low excitation power, as the structure of the crystalline lattice provides an optimal positioning of the luminescence centres within the matrix. Upconverting nanoparticles have no observable photobleaching or blinking, and have recently been used for *in vivo* cell and molecular targeting and imaging[59,60]. However, upconverting nanoparticles require a surface coating to shield biological tissues from toxic lanthanide ions. In addition, they have broad emission spectra, which limits the flexibility for multi-label imaging.

SERS nanoparticles. SERS nanoparticles are composed of specific organic Raman reporter molecules that are attached to the surface of metallic nanoparticles (for example, silver or gold nanoparticles) (reviewed in REFS 61,62). At the resonance frequency of these metallic nanoparticles, strong electromagnetic coupling between the nanoparticle and the reporter molecule produces a characteristic

Multiphoton
All photonic processes depend nonlinearly on light intensity. Multiphoton microscopy takes advantage of such nonlinear processes as a source of contrast.

Fluorescence decay after photoactivation or photoconversion
(FDAP). An imaging assay that is similar to traditional fluorescence recovery after photobleaching (FRAP) but that uses photoactivatable (or photoconvertible) proteins as labelling molecules. The added benefit of visualizing only a limited population of photoactivated or photoconverted molecules is that this avoids the very high laser powers that are necessary to carry out FRAP experiments. It also enables the analysis of the diffusion behaviour and turn-over of photoactivated or photoconverted molecules independently of other proteins that are newly synthesized.

SERS spectrum that can be detected using laser Raman spectrometry or SERS microscopy. Functionalized SERS nanoparticles have no toxic effects in biological tissue and have been used in a targeted multi-label imaging modality *in vivo*[63,64], as each SERS reporter has a unique spectral signature. However, SERS nanoparticles have a marked blinking behaviour.

SHG nanoprobes. SHG nanoprobes are inorganic nanocrystals consisting of noble metals or metal oxides that are arranged in a non-centrosymmetric crystal structure (reviewed in REF. 65). They can generate a second harmonic signal under the intense illumination of a multiphoton microscope by converting two photons into one photon of half the incident wavelength. The optical signal of SHG nanoprobes neither photobleaches nor blinks, and the signal does not saturate with increasing illumination intensity. The signal spectrum of SHG nanoprobes is tunable, which enables various combinations of SHG nanoprobes and fluorescence proteins to be used for imaging. In addition, the signal spectrum is very narrow, which enables imaging in the absence of background noise by using optimized emission filters with very narrow bandwidths. Given that different SHG-capable materials have distinct SHG intensity spectral profiles, different SHG nanoprobes can be readily distinguished, in a so-called 'multi-SHG imaging modality', by comparing relative SHG signal intensities from at least two distinct excitation wavelengths. Recently, physiologically inert barium titanate ($BaTiO_3$) SHG nanoprobes have been applied to whole-animal imaging[50,66] (FIG. 1c).

What all of these non-genetically encoded nanoprobes have in common is that their broader application will crucially depend on their reliable production, proper functionalization and targeted attachment to biological molecules of interest in embryos. This will ensure that engineered nanoprobes can be used as imaging probes for future *in vivo* cellular and molecular dynamic studies, which will eventually enable straightforward single-molecule detection and tracking in whole-embryo imaging. A formidable challenge will be to provide robust bioorthogonal labelling strategies[67] for nanoprobe bioconjugates, thereby securing proper cellular and molecular targeting and retaining full biofunctionality.

Microscopy techniques

To understand the genetic control of embryonic morphogenesis and how cells proliferate, differentiate and organize into functional structures, developmental biologists were for a long time limited to static and two-dimensional analyses of fixed embryos. In the past two decades, the emergence of sophisticated microscopy techniques has opened the field to three-dimensionally resolved, dynamic and long-term *in vivo* imaging. As embryos are often small enough for optical imaging, fluorescence microscopy became the method of choice for both structural and functional imaging of live embryos in combination with quantitative analyses. The seminal but laborious efforts of John Sulston and colleagues in the 1980s to map embryonic cell lineages[3] can now be efficiently recapitulated with automated lineage tracing in entire, live worm embryos using standard confocal microscopy[68]. However, the unique characteristics of live embryos still pose a formidable challenge to current microscopy techniques: their inner structure is inhomogeneous and constantly moving; they can be highly sensitive to manipulation and photodamage; and their morphogenetic processes can occur at a wide range of temporal and spatial scales. In this context, recent developments in multiphoton and light-sheet microscopy hold great promise for multidimensional and multiscale whole-embryo imaging.

Multiphoton microscopy. To capture single-cell dynamics inside living embryos, imaging depth into the tissue is often the main limitation of microscopy. The depth at which images can be recorded with sufficient quality is limited by the optical properties of embryonic tissues. These properties depend on the species and vary in time and space during development[69]. The most effective approach for deep-tissue fluorescence imaging is two-photon excited fluorescence microscopy[70] (BOX 1; TABLE 2), which has been successfully used to investigate cell population dynamics in various embryonic model systems, including fly[71–73], quail[74] and mouse[75,76]. For example, two-photon microscopy has enabled the study of diffusion properties within the highly scattering yolk of fly embryos[77]. Similarly, the large-scale dynamics of the deepest mesoderm cells during fly gastrulation have been followed using two-photon microscopy[72] (FIG. 1e).

An attractive feature of multiphoton microscopy is its ability to carry out label-free imaging (without the need for fluorescent probes) of embryos using additional, nonlinear contrast mechanisms. In particular, harmonic generation signals, such as SHG and third-harmonic generation (THG), from lipid bodies[78], cell interfaces[79], mitotic spindles[79] or muscles[80] enable structural imaging of unstained embryos, without the limitation of photobleaching, and can be directly combined with fluorescence. Such intrinsic contrast has been used recently to reconstruct cell lineages and to study cell division patterns in early zebrafish embryos[79] (FIG. 1f). In addition, a unique advantage of multiphoton imaging is its straightforward application for spatially confined photomanipulation inside embryos, including precise photoablation[71,81] or photoactivation of proteins[31,33].

Among recent improvements of multiphoton microscopy, the ability to reach longer excitation wavelengths with improved laser sources opens up new opportunities for whole-embryo imaging: moving from an excitation wavelength of 800 nm to the 1,200–1,500 nm range provides sufficient energy for the excitation of imaging probes in the red and near-infrared spectra, with increased optical penetration and decreased photodamage[80] (BOX 1). In addition, reaching such wavelengths by combining the conventional titanium-sapphire laser with an optical parametric oscillator offers the ability to improve multicolour, multiphoton imaging by mixing excitation wavelengths. Using this methodology, simultaneous, efficient and independent two-photon excitation of multiple fluorophores in live Brainbow-labelled tissues and

Blinking
Large intensity fluctuation between a bright state (On) and a dark state (Off) of an imaging probe that is under continuous excitation.

Raman reporter molecules
Nitrogen-containing cationic dyes, sulphur-containing dyes or thio-small molecules, which can inelastically scatter a fraction of the absorbed light into a series of different wavelengths that are indicative of the vibrational transitions in the molecules.

Bioorthogonal labelling
Labelling reactions that can occur inside living embryos without interfering with the native biological system.

Harmonic generation
A coherent contrast mechanism that relies on nonlinear scattering of light. Unlike fluorescence, second-harmonic generation (SHG) and third-harmonic generation (THG) do not involve light absorption.

Optical parametric oscillator
An optical device that converts an input laser wave into an output wave of a lower frequency (or greater wavelength). The one used in multiphoton microscopy is pumped by a standard titanium-sapphire laser in the 750–900 nm range, which enables output wavelengths to reach the 1,000–1,500 nm range.

Conformal scanning
Unlike raster scanning, which is used in most point-scanning microscopes, conformal scanning uses a laser scanning pattern that is adapted to the sample shape.

Dynamic aberration correction
An experimental procedure to correct for changing optical aberrations that are induced by embryonic tissues during development using adaptive optics and real-time corrections.

embryos was recently demonstrated[82]. Future progress in laser scanning microscopy will certainly benefit from the improved ability to tailor illumination and detection parameters at each point of the embryo and actively adapt them to the changing properties of developing organisms, as exemplified by conformal scanning that has been adjusted to the embryo shape[79] or dynamic aberration correction in live embryos[83].

Light-sheet microscopy. Although these advances in multiphoton microscopy hold great promise for expanding our knowledge of how an organism develops, we still face challenges to truly appreciate the dynamic nature of a developing living organism with sufficient spatiotemporal resolution. Recording embryonic development in multiple dimensions and scales often defies the speed performance of conventional microscopes. Both standard confocal and two-photon microscopes rely on point scanning: images are recorded one pixel at a time, resulting in pixel rates below 1 MHz (<10^6 pixels per second). However, much higher pixel rates are required to capture fast processes, including beating heart development[84,85], fluid flow dynamics[81,86] and cilia motility[87]. In addition, high-speed imaging is required for the multiscale investigation of slower processes, such as cell migration, shape changes or proliferation. To improve imaging speed, the past decade has seen the emergence of light-sheet microscopy as the most promising microscopy technique for fast, volumetric imaging of live embryos[88]. The ability to carry out fast, three-dimensional optical sectioning with both an extended field of view and limited photodamage is a unique advantage of light-sheet microscopy (BOX 2; TABLE 2). It has enabled the whole-embryo imaging of early zebrafish embryos with a sufficient pixel rate (>100 MHz) and spatial resolution to track in parallel thousands of cells during the first 24 hours of zebrafish development[89]. Recently, the favourable characteristics of light-sheet microscopy were beautifully illustrated by monitoring the activity of a large-scale ensemble of neurons in larval zebrafish[90,91]. By using a vertical sample holder, which enables the embryo to be easily rotated and imaged from different angles, a better image quality[92,93], an isotropic spatial resolution[94] and a further improvement in imaging speed[93,95,96] can be attained.

However, the imaging speed of light-sheet microscopy comes with several limitations for whole-embryo imaging, including uneven image quality and limited imaging depth (BOX 2). These properties compromise intensity-based measurements and deep-tissue imaging,

Table 2 | **Properties to consider when choosing microscopy techniques for whole-embryo imaging**

Properties	Confocal microscopy	Multiphoton microscopy	Light-sheet microscopy*	Advanced light-sheet microscopy‡
Standard imaging speed (pixel rate)	<1 MHz	<1 MHz§	>10–100 MHz	>10–100 MHz
Standard spatial resolution	<0.4 µm (lateral) and <2 µm (axial)	<0.5 µm (lateral)‖ and <3 µm (axial)¶	<0.5 µm (lateral)# and <3 µm (axial)**	Up to <0.5 µm (lateral) and up to <0.5 µm (axial)
Imaging depth‡‡	Limited	Best	Limited	Improved
Photodamage (photobleaching and phototoxicity)§§	Strong	Medium‖‖	Low	Low
Detection	Point detector	Point detector	Widefield detector	Widefield detector
Sample preparation	Standard for upright and inverted microscope	Standard for upright and inverted microscope	Unusual mounting procedure that depends on the geometry of the scope (needs access from at least two orthogonal directions)	Unusual mounting procedure that depends on the geometry of the scope (needs access from at least two orthogonal directions)
Commercial availability	Yes	Yes	Yes	No
Main limitations	Imaging speed, imaging depth and photodamage	Imaging speed and potential nonlinear photodamage	Imaging depth and inhomogeneity of image quality	Advances are not yet commercially available
Main advantages	Accessible in most imaging facilities	Imaging depth	Combined imaging speed, large field of view, low photodamage and quasi-isotropic spatial resolution can be obtained	Optimal compromise between signal to noise ratio, imaging speed, field of view, spatial resolution, imaging depth and photodamage

*Commercially available (using Gaussian beam illumination and one-photon excited fluorescence). ‡With recent developments, such as confocal detection, multiphoton excitation or Bessel beam illumination. §Using the same labelling method and specimen type as confocal microscopy. The pixel rate is in principle slightly lower than with confocal microscopy owing to lower signal levels; however, as multiphoton microscopy is better at imaging at greater depth, the pixel rate can be similar or higher when imaging deep into light-scattering embryos. ‖Lateral spatial resolution is in principle lower than for confocal microscopy owing to longer excitation wavelengths; however, this resolution is maintained at a depth that is unreachable with confocal or light-sheet microscopy. ¶Axial resolution is strongly degraded in depth with all techniques; multiphoton microscopy is better suited for maintaining good axial resolution deep into light-scattering embryos. #Lateral resolution is more sensitive to light scattering and aberration in the detection path than with other techniques. **Axial resolution depends on the thickness of the light sheet and is not even within the field of view. ‡‡Absolute depth of imaging strongly depends on the optical properties of the embryo. §§This is representative, as photodamage strongly depends on labelling method, specimen type and fine-tuning of acquisition parameters. ‖‖Nonlinear photodamage can occur in multiphoton microscopy and can be minimized by adjusting excitation parameters, such as the laser pulse width, repetition rate or wavelength.

Box 2 | **Increased imaging speed but limited imaging depth and image quality in light-sheet microscopy**

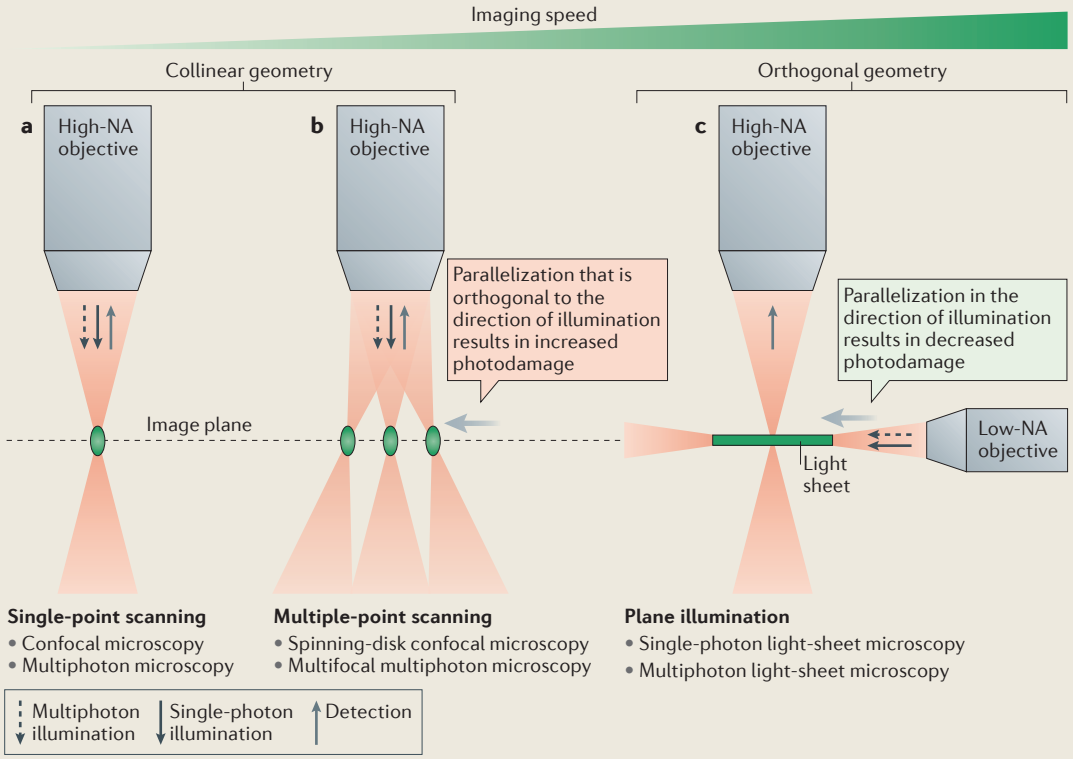

Both confocal and multiphoton microscopes rely on single-point scanning and record images one pixel at a time (see the figure, part **a**), which provides slow imaging speed. To improve acquisition speed, the most effective strategy is to parallelize illumination and detection: starting with spinning-disk confocal microscopy, in which several discrete points are illuminated at a time (see the figure, part **b**), and progressing to the ultimate parallelization by light-sheet microscopy, in which the entire imaging plane is illuminated at once (see the figure, part **c**). In this case, a sheet of light is generated either using a cylindrical lens[88] or by scanning a weakly focused Gaussian beam[89,97], and imaged with a camera oriented orthogonally to the sheet. In light-sheet microscopy, the optical sectioning is due to the confinement of the fluorescence excitation within the illuminated sheet. Such illumination induces less photodamage. Compared with the collinear geometry of most microscopes (see the figure, parts **a**,**b**), the orthogonal geometry of light-sheet microscopes (see the figure, part **c**) results in decreased out-of-focus excitation and the parallelization of illumination along the light propagation direction, which reuses the same excitation energy. In multifocal approaches (see the figure, part **b**), the illuminating beam is split and highly focused, which uses more energy with stronger intensities and induces out-of-focus excitation.

Limited imaging depth and uneven image quality in terms of signal and spatial resolution throughout the field of view are two current limitations of light-sheet microscopy. Most light-sheet microscopes have a Gaussian light-sheet profile, which results in uneven axial resolution (better resolution in the image centre than at the edges). Gaussian beam illumination also imposes a compromise between axial resolution and field of view size: less focusing of the excitation beam results in a larger field of view but a thicker light sheet with degraded axial sectioning. The signal level is also sensitive to aberrations and absorption along the path of illumination propagation, often resulting in images with striped features along the illumination axis. Finally, light scattering when imaging deep into embryos quickly degrades axial resolution and increases background noise levels: the thickness of the light sheet increases with depth, and scattered emitted photons contribute to the image background noise. Substantial efforts by many microscopy laboratories are currently directed towards addressing these issues.

The ability to gather light is indicated by the numerical aperture (NA).

Gaussian beam
The intensity profile of a laser beam after focusing it with a standard microscope objective.

Bessel beam
A specific laser beam profile with elongated axial and short lateral extensions of the focal volume.

which are crucial requirements for future quantitative animal studies. To address these shortcomings, several approaches using multiphoton[97,98], Bessel beam[99,100] or multidirectional[101] illumination have recently succeeded in improving either the penetration depth of the light sheet or the homogeneity of fluorescence excitation, and the spatial resolution throughout the field of view. For example, multiphoton light-sheet microscopy enabled both fast and deep imaging of live fly embryos with the additional benefit of decreased photodamage compared with standard multiphoton microscopy[97]. In terms of detection, the imaging depth of light-sheet microscopy is restricted by scattered photons that contribute to background noise. Among recently tested strategies to remove the background signal[102–104] (FIG. 1g), confocal slit detection seems to provide the fastest acquisition speed and is the most straightforward to implement[105,106]. Although these approaches are neither fully mature nor commercially

available yet, they reflect the active field of research to improve light-sheet microscopy. Recent initiatives to provide open access technology platforms will certainly help in disseminating this technique and its recent advances to the developmental biology community[107,108].

Quantitative tools for processing and analysis

Advances in imaging probes and microscopy techniques have provided improved detection sensitivity with higher spatiotemporal resolution, larger fields of view and lower photodamage within entire living embryos. However, the size and multidimensional and multiscale nature of the resulting digital imaging data often hamper thorough investigation. To cope with the amount and complexity of data, and to gain insights into the molecular and structural dynamics of living biology, computer-based image processing and quantitative image analysis are necessary but remain a bottleneck in research. A typical quantitative analysis workflow for whole-embryo imaging includes image filtering and reconstruction, visualization, segmentation and registration, or feature computation and analysis[109,110]. Such quantitative tools help to visualize, explore and interact with the multidimensional imaging data. They are crucial to feed theoretical models, implement high-throughput strategies and gain new biological insights that would be impossible to obtain otherwise. Recent quantitative imaging of live embryos has proved its potential to investigate embryonic development, with applications in morphogen gradient formation[14–20], transcription factor dynamics[31], cell lineage analysis[68], tissue morphogenesis[72] and quantitative *in vivo* phenotyping[111]. In parallel, large-scale advances in computer vision and bioimage informatics in the past decade have resulted in crucial software developments for the visualization, processing and analysis of multidimensional biological imaging data, with both commercial software and open-source options[112]. However, the case studies that are used to develop such informatics tools rarely focus on live-embryo imaging data and are usually limited to static, three-dimensional approaches. The visualization-assisted analysis system V3D[113] and the virtual brain explorer for zebrafish (ViBE-Z) software[114] are powerful tools that have been successfully applied to visualize, analyse or register complex three-dimensional neuronal tissue structures. In light of such promising developments, there is an overall consensus that quantitative computational analysis tools and imaging workflows need to be generalized and standardized to comprehensively capture dynamic developmental processes[109,110,115,116]. Here, we address this formidable task by discussing the challenges in three major areas — visualization, imaging data registration and feature computation — to accomplish a truly systematic workflow for the processing and analysis of whole-embryo imaging data.

Visualization. Embryonic development is fundamentally a multidimensional and multiscale process. Both commercial and open-source software have made important progress in the past decade for rendering and visualizing multidimensional data, including space, time and colour dimensions. However, in practice, investigators are often faced with the difficult task of visualizing the experimental workflow at all levels: from raw whole-embryo image acquisition to graph or figure design for article publication. For example, when cells are moving within a densely packed three-dimensional tissue, visualization and exploration of the imaging data sets is challenging even with the best available visualization tools. As a consequence, these tools should not only handle the large size of imaging data sets obtained with advanced microscopy techniques but also should help researchers to explore, interact with and understand complex data.

Despite the multidimensional nature of embryonic development, in some cases the dimensionality of the biological process can be reduced without losing crucial information. For example, in the case of morphogen gradient formation in the fly wing, most molecules are restricted to the most apical region of the wing imaginal disc epithelium, which is composed of a single cell-layer sheet. This tissue geometry and subcellular morphogen distribution have enabled investigators to analyse the gradient in two dimensions by projecting optical sections that encompass the apical domain onto a single plane[14]. Similarly, projecting the fluorescent signal and unwrapping the cell tracks from four-dimensional imaging data to two-dimensional maps have recently been applied to follow cell movements or cell shape changes during the early stages of fly[117] or zebrafish[96] development (FIG. 1h).

However, such direct projection of imaging data and smart use of embryonic geometry to reduce dimensionality are often stage-, process- and species-specific approaches and are not always possible, in which case visualization tools are required to help to break down the complexity. For example, the V3D software[113] aids the understanding of three-dimensional gene expression patterns by displaying gene expression profiles along lines that have been interactively drawn by the user. A spatial coordinate system, which has been adapted to the shape of the embryonic tissue, can also be used to decompose, visualize and comprehend complex three-dimensional cell movements according to their biologically relevant components[72]. The investigation of several stereotypical and fundamental morphogenetic events, such as cell intercalation, would greatly benefit from the design of specific visualization tools. It is currently very challenging to visualize and identify cell intercalations that occur in all dimensions deep within an embryo. To this end, visualization tools could take advantage of the specific geometry of both planar and radial cell intercalations[118] to carry out local projections and to explore large imaging data sets. These examples strikingly illustrate how quantitative tools can help developmental biologists to visualize multidimensional whole-embryo imaging data by breaking down complexities. Obviously, such tools will need to be generalized in the future. A recent, fully multidimensional approach to quantitatively phenotype cell movements in the early worm embryo using three-dimensional representations — although it is limited to a small number of cells — is a promising advance in data visualization[111].

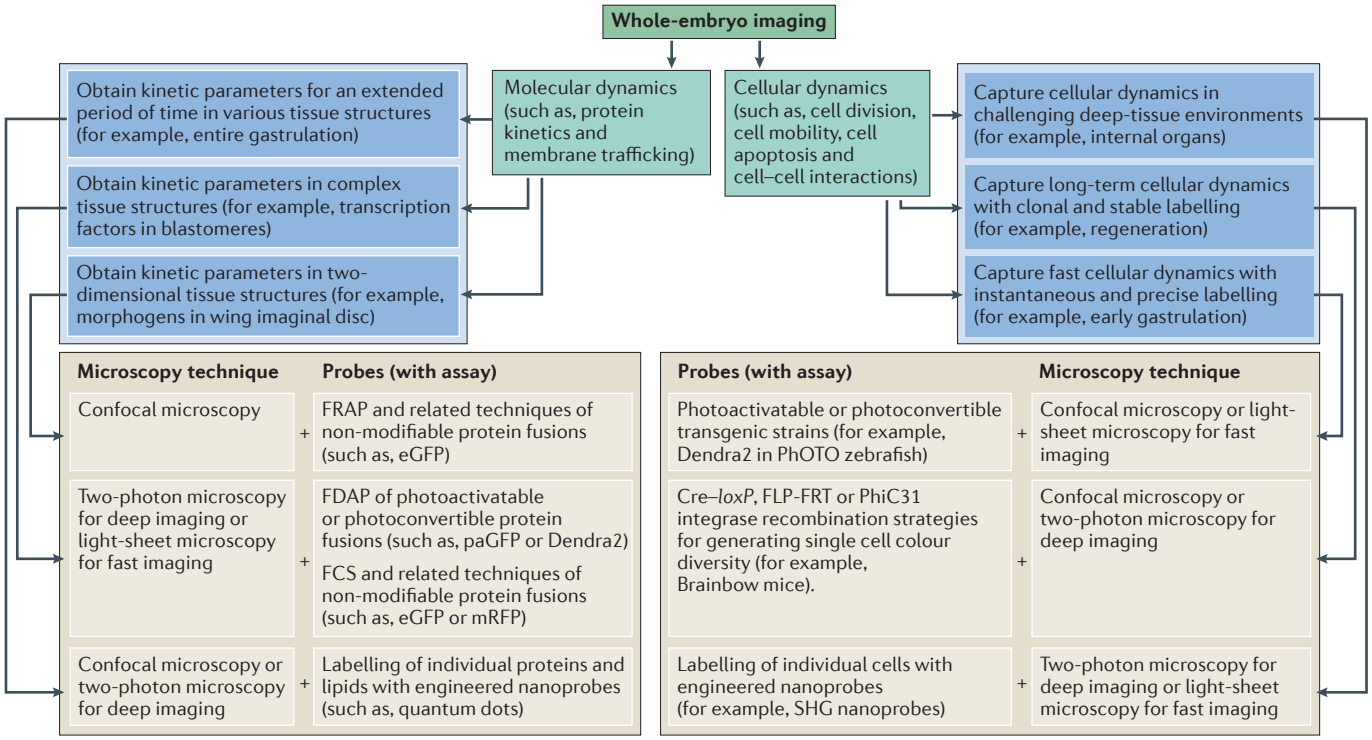

Figure 2 | **Quantitative whole-embryo imaging: a selection flowchart for specific applications in cellular and molecular dynamics.** The selection flowchart provides a comprehensive overview by specifying the main examples of applications, questions or problems (summarized in blue and green boxes), and by suggesting present and future imaging probes and microscopy techniques (summarized in beige boxes) for carrying out quantitative imaging studies during development. Only passive labels are considered as probes, excluding biosensors, optogenetic actuators and sensors. To capture cellular dynamics in deep-tissue environments, the currently available fluorescent proteins are of limited use owing to photobleaching and signal saturation. The detailed qualities of imaging probes and microscopy techniques are discussed in TABLE 1 and TABLE 2, respectively. Fluorescence recovery after photobleaching (FRAP)-related techniques include fluorescence localization after photobleaching (FLAP) and fluorescence loss in photobleaching (FLIP). Fluorescence correlation spectroscopy (FCS)-related techniques include fluorescence cross-correlation spectroscopy (FCCS) and image correlation spectroscopy (ICS). The PhiC31 integrase efficiently recombines sequences that contain attB sites with sequences containing attP sites. eGFP, enhanced GFP; FDAP, fluorescence decay after photoactivation or photoconversion; FLP, flippase; FRT, flippase recognition target; mRFP, monomeric red fluorescent protein; paGFP, photoactivatable GFP; PhOTO zebrafish, photoconvertible optical tracking of zebrafish; SHG, second harmonic generation.

Imaging data registration. Registration corresponds to any transformation that is applied to the imaging data to enable data from different experiments to be combined or compared. This task is crucial to investigate the variability between individual embryos, to carry out statistical analyses and to ensure the reproducibility of experimental data. Registration encompasses many procedures, including image reconstruction, alignment or stitching, drift correction, time synchronization or the definition of a coordinate system that has been adapted to the body plan. Building canonical digital atlases from different experiments is a powerful tool to investigate the complexity of signalling or morphological patterns. To combine data and to overcome variations in morphology or patterning between individuals, inter-specimen registration has been used to map stereotypical cell locations in worms[119] or gene expression patterns in flies[120] into canonical digital atlases. More recently, the ViBE-Z software[114] introduced an automated registration procedure, which uses trainable landmark detection, reorientation of the imaging data and elastic deformation to align three-dimensional maps of gene expression patterns in the zebrafish larval brain into anatomical reference models. Such efforts provide the possibility to gain new insights by combining multiple experiments, such as virtual colocalization of gene expression patterns. However, it will be essential to extend these approaches to live imaging data that encompass molecular and cellular dynamics. Such registrations of multi-dimensional, dynamic imaging data can provide a deeper understanding of variability beyond the static canonical patterns, potentially identifying stereotypical and non-stereotypical dynamics during development.

Quantitative feature computation. Feature computation is a crucial step to obtain biological insights from imaging data. These features are quantitative descriptors that are extracted from the images and that describe signalling patterns or embryonic morphogenesis. New tools are emerging to quantify biological features that are

specific to embryonic development, such as morphogen gradients, cell movement, cell division, cell intercalation, tissue invagination or convergence extension at the level of the whole embryo[109]. Cell lineage reconstruction illustrates the potential of feature computation in whole-embryo imaging: it relies on three-dimensional cell tracking and identification of cell division by using *in vivo* recording of embryonic development to investigate cell fate[68]. Usually, fluorescent labelling of nuclei[68,116] is used, but label-free (SHG and THG) microscopy in zebrafish embryos has also been accomplished[79]. Quantitative measures of molecular signalling and morphology recently revealed how coordinated morphogen gradients and cell motion establish tissue patterning during zebrafish neural tube formation[121]. However, feature computation in whole-embryo imaging remains a difficult task, as the quantitative investigation of morphogenesis is often limited to manual investigation. Image segmentation and cell tracking are typically carried out or corrected manually, and quantitative measurements rely on visual inspections. Evidently, the current workflow is not compatible with the analysis of large data sets in whole-embryo imaging. In addition, standard metrics are lacking for the quantification of many stereotypical features of embryonic morphogenesis, such as cell intercalation and tissue invagination. There is a need for automated approaches, expansion of segmentation tools and standard metrics. For example, cell membrane segmentation is crucial for investigating tissue morphogenesis or cell shape changes and can provide better accuracy for tracking cells *in vivo*. Efficient and automated three-dimensional membrane segmentation tools in live embryos are only now being developed[122,123]. In the near future, automated computation of multiple features by standard protocols will enable researchers to fully benefit from the rich content of whole-embryo images.

Conclusions

The imaging 'toolbox' that is available to developmental biologists has expanded markedly during the past decade. Embryonic development can now be investigated *in vivo* with improved spatiotemporal resolution, at multiple scales and with more detailed quantitative analyses. More specifically, the application of a diverse set of genetically encoded proteins has enabled molecular dynamics inside living embryos to be investigated with sophisticated quantitative analyses, including FCS, FRAP or FDAP. The emergence of proteins with near-infrared emission spectra and engineered nanoprobes with superior optical characteristics is poised to overcome the current limitations of fluorescent probes, which will create new opportunities to investigate development in unprecedented detail. In addition, recent applications and innovations in multiphoton and light-sheet microscopy are moving the field towards deeper and faster *in vivo* whole-animal imaging with reduced photodamage, which will ultimately enable truly multi-dimensional and multiscale investigations of embryonic development. Finally, whole-embryo image processing and analyses face challenges including visualization, data registration and feature computation, but there have been recent promising advances in these areas. The integration of such imaging tools to deliver a better understanding of the principles of development will demand a coordinated interdisciplinary effort. Developmental biologists will increasingly need to carry out and design experimental approaches in close interaction with chemists (for probe development and functionalization), engineers (for image modality refinement), biophysicists (for modelling) and computer scientists (for data management and image analyses). In addition, developmental biologists need to critically evaluate new imaging tools, as it is often difficult to predict whether innovations are mature enough to be useful beyond the 'proof of principle'. Here, we provide a general selection framework to the reader with advice to help choose adapted tools for future cellular and molecular dynamic studies in whole-embryo imaging on the basis of recent literature and our own experience (FIG. 2; TABLES 1,2). An exchange platform can further facilitate the identification of the right tools for the desired experimental purpose. To this end, recently established imaging platforms (such as BioEmergences[110]), networks of core facilities (such as Core for Life[124]) and 'open hardware' initiatives (such as OpenSPIM[107]) are encouraging first steps to promote this much-needed exchange. In light of these advances, developmental biologists enter an exciting time to tackle the formidable challenge of exploring the complexities of life.

1. Lewis, E. B. A gene complex controlling segmentation in *Drosophila*. *Nature* **276**, 565–570 (1978).
2. Nüsslein-Volhard, C. & Wieschaus, E. Mutations affecting segment number and polarity in *Drosophila*. *Nature* **287**, 795–801 (1980).
3. Sulston, J. E., Schierenberg, E., White, J. G. & Thomson, J. N. The embryonic cell lineage of the nematode *Caenorhabditis elegans*. *Dev. Biol.* **100**, 64–119 (1983).
4. Oates, A. C., Gorfinkiel, N., González-Gaitán, M. & Heisenberg, C.P. Quantitative approaches in developmental biology. *Nature Rev. Genet.* **10**, 517–530 (2009).
5. Mavrakis, M., Pourquié, O. & Lecuit, T. Lighting up developmental mechanisms: how fluorescence imaging heralded a new era. *Development* **137**, 373–387 (2010).
6. Miyawaki, A. Proteins on the move: insights gained from fluorescent protein technologies. *Nature Rev. Mol. Cell. Biol.* **12**, 656–668 (2011).
7. Muller, P., Rogers, K. W., Yu, S. R., Brand, M. & Schier, A. F. Morphogen transport. *Development* **140**, 1621–1638 (2013).
8. Nienhaus, K. & Ulrich Nienhaus, G. Fluorescent proteins for live-cell imaging with super-resolution. *Chem. Soc. Rev.* **43**, 1088–1106 (2013).
9. Prasher, D. C., Eckenrode, V. K., Ward, W. W., Prendergast, F. G. & Cormier, M. J. Primary structure of the *Aequorea victoria* green-fluorescent protein. *Gene* **111**, 229–233 (1992).
10. Chalfie, M., Tu, Y., Euskirchen, G., Ward, W. W. & Prasher, D. C. Green fluorescent protein as a marker for gene expression. *Science* **263**, 802–805 (1994).
11. Zacharias, D. A., Violin, J. D., Newton, A. C. & Tsien, R. Y. Partitioning of lipid-modified monomeric GFPs into membrane microdomains of live cells. *Science* **296**, 913–916 (2002).
12. Axelrod, D., Koppel, D. E., Schlessinger, J., Elson, E. & Webb, W. W. Mobility measurement by analysis of fluorescence photobleaching recovery kinetics. *Biophys. J.* **16**, 1055–1069 (1976).
13. Magde, D., Elson, E. & Webb, W. Thermodynamic fluctuations in a reacting system—measurement by fluorescence correlation spectroscopy. *Phys. Rev. Lett.* **29**, 705–708 (1972).
14. Kicheva, A. *et al.* Kinetics of morphogen gradient formation. *Science* **315**, 521–525 (2007). **Analyses the kinetic parameters of Decapentaplegic (Dpp) and Wingless (Wg) morphogen gradient formation using FRAP. Provides evidence that endocytosis is required for Dpp spreading.**
15. Gregor, T., Wieschaus, E. F., McGregor, A. P., Bialek, W. & Tank, D. W. Stability and nuclear dynamics of the bicoid morphogen gradient. *Cell* **130**, 141–152 (2007).
16. Yu, S. R. *et al.* Fgf8 morphogen gradient forms by a source-sink mechanism with freely diffusing molecules. *Nature* **461**, 533–536 (2009).

Analyses the Fgf8 morphogen gradient using FCS. Provides evidence that a freely diffusing Fgf8 morphogen can set up the gradient by a source–sink mechanism.
17. Abu-Arish, A., Porcher, A., Czerwonka, A., Dostatni, N. & Fradin, C. High mobility of bicoid captured by fluorescence correlation spectroscopy: implication for the rapid establishment of its gradient. *Biophys. J.* **99**, L33–L35 (2010).
18. Muller, P. *et al.* Differential diffusivity of Nodal and Lefty underlies a reaction-diffusion patterning system. *Science* **336**, 721–724 (2012).
19. Daniels, B. R., Rikhy, R., Renz, M., Dobrowsky, T. M. & Lippincott-Schwartz, J. Multiscale diffusion in the mitotic *Drosophila melanogaster* syncytial blastoderm. *Proc. Natl Acad. Sci.* **109**, 8588–8593 (2012).
20. Zhou, S. *et al.* Free extracellular diffusion creates the dpp morphogen gradient of the *Drosophila* wing disc. *Curr. Biol.* **22**, 668–675 (2012).
21. Wohland, T., Shi, X., Sankaran, J. & Stelzer, E. H. K. Single Plane Illumination Fluorescence Correlation Spectroscopy (SPIM-FCS) probes inhomogeneous three-dimensional environments. *Opt. Express* **18**, 10627–10641 (2010).
22. Capoulade, J., Wachsmuth, M., Hufnagel, L. & Knop, M. Quantitative fluorescence imaging of protein diffusion and interaction in living cells. *Nature Biotech.* **29**, 835–839 (2011).
23. Livet, J. *et al.* Transgenic strategies for combinatorial expression of fluorescent proteins in the nervous system. *Nature* **450**, 56–62 (2007).
24. Hadjieconomou, D. *et al.* Flybow: genetic multicolor cell labeling for neural circuit analysis in *Drosophila melanogaster*. *Nature Meth* **8**, 260–266 (2011).
25. Kanca, O., Caussinus, E., Denes, A. S., Percival-Smith, A. & Affolter, M. Raeppli: a whole-tissue labeling tool for live imaging of *Drosophila* development. *Development* **141**, 472–480 (2014).
26. Gupta, V. & Poss, K. D. Clonally dominant cardiomyocytes direct heart morphogenesis. *Nature* **484**, 479–484 (2012).
27. Tabansky, I. *et al.* Developmental bias in cleavage-stage mouse blastomeres. *Curr. Biol.* **23**, 21–31 (2013).
References 26 and 27 describe the recent application of lineage tracing that uses rainbow-labelled clones in the growing zebrafish heart and in mouse blastocysts.
28. Dempsey, W. P., Fraser, S. E. & Pantazis, P. PhOTO zebrafish: a transgenic resource for *in vivo* lineage tracing during development and regeneration. *PLoS ONE* **7**, e32888 (2012).
29. Patterson, G. H. & Lippincott-Schwartz, J. A photoactivatable GFP for selective photolabeling of proteins and cells. *Science* **297**, 1873–1877 (2002).
30. Gurskaya, N. G. *et al.* Engineering of a monomeric green-to-red photoactivatable fluorescent protein induced by blue light. *Nature Biotech.* **24**, 461–465 (2006).
31. Plachta, N., Bollenbach, T., Pease, S., Fraser, S. E. & Pantazis, P. Oct4 kinetics predict cell lineage patterning in the early mammalian embryo. *Nature Cell Biol.* **13**, 117–123 (2011).
Uses the FDAP assay to examine the binding kinetics of the pluripotency factor OCT4. Shows that the kinetics of OCT4–chromatin binding predict cell lineage patterning in the early mouse embryo.
32. Kaur, G. *et al.* Probing transcription factor diffusion dynamics in the living mammalian embryo with photoactivatable fluorescence correlation spectroscopy. *Nature Comms* **4**, 1637 (2013).
33. Pantazis, P. & González-Gaitán, M. Localized multiphoton photoactivation of paGFP in *Drosophila* wing imaginal discs. *J. Biomed. Opt.* **12**, 044004 (2007).
34. Pantazis, P. & Bollenbach, T. Transcription factor kinetics and the emerging asymmetry in the early mammalian embryo. *Cell Cycle* **11**, 2055–2058 (2012)
35. Strack, R. L. *et al.* A rapidly maturing far-red derivative of DsRed-Express2 for whole-cell labeling. *Biochemistry* **48**, 8279–8281 (2009).
36. Lin, M. Z. *et al.* Autofluorescent proteins with excitation in the optical window for intravital imaging in mammals. *Chem. Biol.* **16**, 1169–1179 (2009).
37. Morozova, K. S. *et al.* Far-red fluorescent protein excitable with red lasers for flow cytometry and superresolution STED nanoscopy. *Biophys. J.* **99**, L13–L15 (2010).
38. Shcherbo, D. *et al.* Near-infrared fluorescent proteins. *Nature Meth.* **7**, 827–829 (2010).
39. Shu, X. *et al.* Mammalian expression of infrared fluorescent proteins engineered from a bacterial phytochrome. *Science* **324**, 804–807 (2009).
40. Filonov, G. S. *et al.* Bright and stable near-infrared fluorescent protein for *in vivo* imaging. *Nature Biotech.* **29**, 757–761 (2011).
41. Auldridge, M. E., Satyshur, K. A., Anstrom, D. M. & Forest, K. T. Structure-guided engineering enhances a phytochrome-based infrared fluorescent protein. *J. Biol. Chem.* **287**, 7000–7009 (2012).
42. Filonov, G. S. *et al.* Deep-tissue photoacoustic tomography of a genetically encoded near-infrared fluorescent probe. *Angew. Chem. Int. Ed. Engl.* **51**, 1448–1451 (2012).
43. Shcherbakova, D. M. & Verkhusha, V. V. Near-infrared fluorescent proteins for multicolor *in vivo* imaging. *Nature Meth* **10**, 751–754 (2013).
44. Rieger, S., Kulkarni, R. P., Darcy, D., Fraser, S. E. & Köster, R. W. Quantum dots are powerful multipurpose vital labeling agents in zebrafish embryos. *Dev. Dyn.* **234**, 670–681 (2005).
45. Mohan, N., Chen, C.-S., Hsieh, H.-H., Wu, Y.-C. & Chang, H.-C. *In vivo* imaging and toxicity assessments of fluorescent nanodiamonds in *Caenorhabditis elegans*. *Nano Lett.* **10**, 3692–3699 (2010).
46. Igarashi, R. *et al.* Real-time background-free selective imaging of fluorescent nanodiamonds *in vivo*. *Nano Lett.* **12**, 5726–5732 (2012).
47. Lim, S. F. *et al.* *In vivo* and scanning electron microscopy imaging of upconverting nanophosphors in *Caenorhabditis* elegans. *Nano Lett.* **6**, 169–174 (2006).
48. Chatterjee, D. K., Rufaihah, A. J. & Zhang, Y. Upconversion fluorescence imaging of cells and small animals using lanthanide doped nanocrystals. *Biomaterials* **29**, 937–943 (2008).
49. Qian, X. *et al.* *In vivo* tumor targeting and spectroscopic detection with surface-enhanced Raman nanoparticle tags. *Nature Biotech.* **26**, 83–90 (2007).
50. Pantazis, P., Maloney, J., Wu, D. & Fraser, S. E. Second harmonic generating (SHG) nanoprobes for *in vivo* imaging. *Proc. Natl Acad. Sci. USA* **107**, 14535–14540 (2010).
Establishes imaging of SHG nanoprobes in live zebrafish embryos.
51. Michalet, X. *et al.* Quantum dots for live cells, *in vivo* imaging, and diagnostics. *Science* **307**, 538–544 (2005).
52. Akerman, M. E., Chan, W. C. W., Laakkonen, P., Bhatia, S. N. & Ruoslahti, E. Nanocrystal targeting *in vivo*. *Proc. Natl Acad. Sci. USA* **99**, 12617–12621 (2002).
53. Gao, X., Cui, Y., Levenson, R. M., Chung, L. W. K. & Nie, S. *In vivo* cancer targeting and imaging with semiconductor quantum dots. *Nature Biotech.* **22**, 969–976 (2004).
54. Tada, H., Higuchi, H., Wanatabe, T. M. & Ohuchi, N. *In vivo* real-time tracking of single quantum dots conjugated with monoclonal anti-HER2 antibody in tumors of mice. *Cancer Res.* **67**, 1138–1144 (2007).
55. Mochalin, V. N., Shenderova, O., Ho, D. & Gogotsi, Y. The properties and applications of nanodiamonds. *Nature Nanotechnol.* **7**, 11–23 (2011).
56. Bradac, C. *et al.* Observation and control of blinking nitrogen-vacancy centres in discrete nanodiamonds. *Nature Nanotechnol.* **5**, 345–349 (2010).
57. Kuo, Y., Hsu, T. Y., Wu, Y. C. & Chang, H. C. Fluorescent nanodiamond as a probe for the intercellular transport of proteins *in vivo*. *Biomaterials* **34**, 8352–8360 (2013).
58. Haase, M. & Schäfer, H. Upconverting nanoparticles. *Angew. Chem. Int. Ed. Engl.* **50**, 5808–5829 (2011).
59. Chien, Y.-H. *et al.* Near-infrared light photocontrolled targeting, bioimaging, and chemotherapy with caged upconversion nanoparticles *in vitro* and *in vivo*. *ACS Nano* **7**, 8516–8528 (2013).
60. Xing, H. *et al.* Computed tomography imaging-guided radiotherapy by targeting upconversion nanocubes with significant imaging and radiosensitization enhancements. *Sci. Rep.* **3**, 1751 (2013).
61. Qian, X. M. & Nie, S. M. Single-molecule and single-nanoparticle SERS: from fundamental mechanisms to biomedical applications. *Chem. Soc. Rev.* **37**, 912 (2008).
62. Kneipp, J., Kneipp, H. & Kneipp, K. SERS—a single-molecule and nanoscale tool for bioanalytics. *Chem. Soc. Rev.* **37**, 1052–1060 (2008).
63. Zavaleta, C. L. *et al.* Multiplexed imaging of surface enhanced Raman scattering nanotags in living mice using noninvasive Raman spectroscopy. *Proc. Natl Acad. Sci.* **106**, 13511–13516 (2009).
64. Zavaleta, C. L. *et al.* A Raman-based endoscopic strategy for multiplexed molecular imaging. *Proc. Natl Acad. Sci.* **110**, E2288–E2297 (2013).
65. Dempsey, W. P., Fraser, S. E. & Pantazis, P. SHG nanoprobes: Advancing harmonic imaging in biology. *Bioessays* **34**, 351–360 (2012).
66. Culic-Viskota, J., Dempsey, W. P., Fraser, S. E. & Pantazis, P. Surface functionalization of barium titanate SHG nanoprobes for *in vivo* imaging in zebrafish. *Nature Protoc.* **7**, 1618–1633 (2012).
67. Prescher, J. A. & Bertozzi, C. R. Chemistry in living systems. *Nature Chem. Biol.* **1**, 13–21 (2005).
68. Bao, Z. *et al.* Automated cell lineage tracing in *Caenorhabditis elegans*. *Proc. Natl Acad. Sci. USA* **103**, 2707–2712 (2006).
69. Supatto, W., McMahon, A., Fraser, S. E. & Stathopoulos, A. Quantitative imaging of collective cell migration during *Drosophila* gastrulation: multiphoton microscopy and computational analysis. *Nature Protoc.* **4**, 1397–1412 (2009).
70. Denk, W., Strickler, J. H. & Webb, W. W. Two-photon laser scanning fluorescence microscopy. *Science* **248**, 73–76 (1990).
71. Supatto, W. *et al.* *In vivo* modulation of morphogenetic movements in *Drosophila* embryos with femtosecond laser pulses. *Proc. Natl Acad. Sci. USA* **102**, 1047–1052 (2005).
72. McMahon, A., Supatto, W., Fraser, S. E. & Stathopoulos, A. Dynamic Analyses of *Drosophila* Gastrulation Provide Insights into Collective Cell Migration. *Science* **322**, 1546–1550 (2008).
Uses multiphoton microscopy and computational image analysis to image the deepest mesoderm cells and to decompose their complex movements during fly embryonic development.
73. Rebollo, E., Roldan, M. & Gonzalez, C. Spindle alignment is achieved without rotation after the first cell cycle in *Drosophila* embryonic neuroblasts. *Development* **136**, 3393–3397 (2009).
74. Sato, Y. *et al.* Dynamic analysis of vascular morphogenesis using transgenic quail embryos. *PLoS ONE* **5**, e12674 (2010).
75. Squirrell, J. M., Wokosin, D. L., White, J. G. & Bavister, B. D. Long-term two-photon fluorescence imaging of mammalian embryos without compromising viability. *Nature Biotech.* **17**, 763–767 (1999).
76. McDole, K., Xiong, Y., Iglesias, P. A. & Zheng, Y. Lineage mapping the pre-implantation mouse embryo by two-photon microscopy, new insights into the segregation of cell fates. *Dev. Biol.* **355**, 239–249 (2011).
77. Gregor, T. Diffusion and scaling during early embryonic pattern formation. *Proc. Natl Acad. Sci.* **102**, 18403–18407 (2005).
78. Débarre, D. *et al.* Imaging lipid bodies in cells and tissues using third-harmonic generation microscopy. *Nature Meth.* **3**, 47–53 (2006).
79. Olivier, N. *et al.* Cell lineage reconstruction of early zebrafish embryos using label-free nonlinear microscopy. *Science* **329**, 967–971 (2010).
Uses harmonic generation microscopy for label-free imaging and cell lineage reconstruction.
80. Andresen, V. *et al.* Infrared multiphoton microscopy: subcellular-resolved deep tissue imaging. *Curr. Opin. Biotechnol.* **20**, 54–62 (2009).
81. Supatto, W., Fraser, S. E. & Vermot, J. An all-optical approach for probing microscopic flows in living embryos. *Biophys. J.* **95**, L29–L31 (2008).
82. Mahou, P. *et al.* Multicolor two-photon tissue imaging by wavelength mixing. *Nature Meth.* **9**, 815–818 (2012).
83. Olivier, N., Débarre, D. & Beaurepaire, E. Dynamic aberration correction for multiharmonic microscopy. *Opt. Lett.* **34**, 3145–3147 (2009).
84. Liebling, M. *et al.* Rapid three-dimensional imaging and analysis of the beating embryonic heart reveals functional changes during development. *Dev. Dyn.* **235**, 2940–2948 (2006).
85. Arrenberg, A. B., Stainier, D. Y. R., Baier, H. & Huisken, J. Optogenetic control of cardiac function. *Science* **330**, 971–974 (2010).
86. Anton, H. *et al.* Pulse propagation by a capacitive mechanism drives embryonic blood flow. *Development* **140**, 4426–4434 (2013).
87. Hirota, Y. *et al.* Planar polarity of multiciliated ependymal cells involves the anterior migration of basal bodies regulated by non-muscle myosin II. *Development* **137**, 3037–3046 (2010).

88. Huisken, J., Swoger, J., Del Bene, F., Wittbrodt, J. & Stelzer, E. H. K. Optical sectioning deep inside live embryos by selective plane illumination microscopy. *Science* **305**, 1007–1009 (2004).
Seminal work that uses light-sheet microscopy for live embryo imaging.
89. Keller, P. J., Schmidt, A. D., Wittbrodt, J. & Stelzer, E. H. K. Reconstruction of zebrafish early embryonic development by scanned light sheet microscopy. *Science* **322**, 1065–1069 (2008).
90. Ahrens, M. B., Orger, M. B., Robson, D. N., Li, J. M. & Keller, P. J. Whole-brain functional imaging at cellular resolution using light-sheet microscopy. *Nature Meth.* **10**, 413–420 (2013).
91. Panier, T. *et al.* Fast functional imaging of multiple brain regions in intact zebrafish larvae using Selective Plane Illumination Microscopy. *Front. Neural Circuits* **7**, 65 (2013).
92. Preibisch, S., Saalfeld, S., Schindelin, J. & Tomancak, P. Software for bead-based registration of selective plane illumination microscopy data. *Nature Meth.* **7**, 418–419 (2010).
93. Krzic, U., Gunther, S., Saunders, T. E., Streichan, S. J. & Hufnagel, L. Multiview light-sheet microscope for rapid in toto imaging. *Nature Meth.* **9**, 730–733 (2012).
94. Swoger, J., Verveer, P., Greger, K., Huisken, J. & Stelzer, E. H. K. Multi-view image fusion improves resolution in three-dimensional microscopy. *Opt. Express* **15**, 8029–8042 (2007).
95. Tomer, R., Khairy, K., Amat, F. & Keller, P. J. Quantitative high-speed imaging of entire developing embryos with simultaneous multiview light-sheet microscopy. *Nature Meth.* **9**, 755–763 (2012).
References 92 and 94 show the recent application of light-sheet microscopy for whole-embryo imaging.
96. Schmid, B. *et al.* High-speed panoramic light-sheet microscopy reveals global endodermal cell dynamics. *Nature Comms* **4**, 1–10 (2013).
97. Truong, T. V., Supatto, W., Koos, D. S., Choi, J. M. & Fraser, S. E. Deep and fast live imaging with two-photon scanned light-sheet microscopy. *Nature Meth* **8**, 757–760 (2011).
Uses a combination of multiphoton excitation and light-sheet illumination to image fly embryos.
98. Lavagnino, Z., Zanacchi, F. C., Ronzitti, E. & Diaspro, A. Two-photon excitation selective plane illumination microscopy (2PE-SPIM) of highly scattering samples: characterization and application. *Opt. Express* **21**, 5998–6008 (2013).
99. Planchon, T. A. *et al.* Rapid three-dimensional isotropic imaging of living cells using Bessel beam plane illumination. *Nature Meth* **8**, 417–423 (2011).
100. Fahrbach, F. O., Gurchenkov, V., Alessandri, K., Nassoy, P. & Rohrbach, A. Self-reconstructing sectioned Bessel beams offer submicron optical sectioning for large fields of view in light-sheet microscopy. *Opt. Express* **21**, 11425 (2013).
101. Huisken, J. & Stainier, D. Y. R. Even fluorescence excitation by multidirectional selective plane illumination microscopy (mSPIM). *Opt. Lett.* **32**, 2608–2610 (2007).
102. Keller, P. J. *et al.* Fast, high-contrast imaging of animal development with scanned light sheet-based structured-illumination microscopy. *Nature Meth.* **7**, 637–642 (2010).
103. Mertz, J. & Kim, J. Scanning light-sheet microscopy in the whole mouse brain with HiLo background rejection. *J. Biomed. Opt.* **15**, 016027 (2010).
104. Gao, L. *et al.* Noninvasive imaging beyond the diffraction limit of 3D dynamics in thickly fluorescent specimens. *Cell* **151**, 1370–1385 (2012).
105. Silvestri, L., Bria, A., Sacconi, L., Iannello, G. & Pavone, F. S. Confocal light sheet microscopy: micron-scale neuroanatomy of the entire mouse brain. *Opt. Express* **20**, 20582–20598 (2012).
106. Baumgart, E. & Kubitscheck, U. Scanned light sheet microscopy with confocal slit detection. *Opt. Express* **20**, 21805–21814 (2012).
107. Pitrone, P. G. *et al.* OpenSPIM: an open-access light-sheet microscopy platform. *Nature Meth.* **10**, 598–599 (2013).
108. Gualda, E. J. *et al.* OpenSpinMicroscopy: an open-source integrated microscopy platform. *Nature Meth.* **10**, 599–600 (2013).
109. Truong, T. V. & Supatto, W. Toward high-content/high-throughput imaging and analysis of embryonic morphogenesis. *Genesis* **49**, 555–569 (2011).
110. Mikut, R. *et al.* Automated processing of zebrafish imaging data: a survey. *Zebrafish* **10**, 401–421 (2013).
111. Moore, J. L., Du, Z. & Bao, Z. Systematic quantification of developmental phenotypes at single-cell resolution during embryogenesis. *Development* **140**, 3266–3274 (2013).
112. Eliceiri, K. W. *et al.* Biological imaging software tools. *Nature Meth.* **9**, 697–710 (2012).
113. Peng, H., Ruan, Z., Long, F., Simpson, J. H. & Myers, E. W. V3D enables real-time 3D visualization and quantitative analysis of large-scale biological image data sets. *Nature Biotech.* **28**, 348–353 (2010).
114. Ronneberger, O. *et al.* ViBE-Z.: a framework for 3D virtual colocalization analysis in zebrafish larval brains. *Nature Meth.* **9**, 735–742 (2012).
115. Khairy, K. & Keller, P. J. Reconstructing embryonic development. *Genesis* **49**, 488–513 (2011).
116. Amat, F. & Keller, P. J. Towards comprehensive cell lineage reconstructions in complex organisms using light-sheet microscopy. *Develop. Growth Differ.* **55**, 563–578 (2013).
117. Blanchard, G. B. *et al.* Tissue tectonics: morphogenetic strain rates, cell shape change and intercalation. *Nature Meth.* **6**, 458–464 (2009).
118. Walck-Shannon, E. & Hardin, J. Cell intercalation from top to bottom. *Nature Rev. Mol. Cell. Biol.* **15**, 34–48 (2014).
119. Long, F., Peng, H., Liu, X., Kim, S. K. & Myers, E. A. 3D digital atlas of *C. elegans* and its application to single-cell analyses. *Nature Meth.* **6**, 667–672 (2009).
120. Fowlkes, C. C. *et al.* A quantitative spatiotemporal atlas of gene expression in the *Drosophila* Blastoderm. *Cell* **133**, 364–374 (2008).
121. Xiong, F. *et al.* Specified neural progenitors sort to form sharp domains after noisy shh signaling. *Cell* **153**, 550–561 (2013).
Shows how quantitative image analysis of both molecular signalling and cell motion provides new insights into tissue patterning.
122. Mosaliganti, K. R., Noche, R. R., Xiong, F., Swinburne, I. A. & Megason, S. G. ACME: automated cell morphology extractor for comprehensive reconstruction of cell membranes. *PLoS Comput. Biol.* **8**, e1002780 (2012).
123. Pop, S. *et al.* Extracting 3D cell parameters from dense tissue environments: application to the development of the mouse heart. *Bioinformatics* **29**, 772–779 (2013).
124. Meder, D. & Van Minnebruggen, G. Straight talk with…Doris Meder and Geert Van Minnebruggen. Interview by Katharine Sanderson. *Nature Med.* **19**, 802 (2013).
125. Wang, X. *et al.* Non-blinking semiconductor nanocrystals. *Nature* **459**, 686–689 (2009).

Acknowledgements
The authors thank former and present members of their laboratories for discussions and feedback during the preparation of this Review. The authors apologize to those whose work could not be discussed owing to space limitations.

Competing interests statement
The authors declare competing interests: see Web version for details.

FURTHER INFORMATION
BioEmergences: http://bioemergences.iscpif.fr
Core for Life: http://www.coreforlife.eu
OpenSPIM: http://openspim.org

ALL LINKS ARE ACTIVE IN THE ONLINE PDF